Lateral variations in the platinum-group element content and mineralogy of the UG2 Chromitite Layer, Bushveld Complex

C.J. Penberthy
Mineralogy Division, Mintek, Private Bag X3015, Randburg, 2125 Republic of South Africa
E-mail: inap@mintek.co.za

R.K.W. Merkle
Applied Mineralogy Group, Department of Geology, University of Pretoria, Pretoria, 0002 Republic of South Africa
E-mail: rkwm@scientia.up.ac.za

Accepted 16 February 1999

Abstract — Investigation of a number of samples of UG2 Chromitite from the Brits–Marikana area revealed significant mineralogical variations. Most of the deviations from typical UG2 can be attributed to interaction with fluids at intermediate to low temperatures, sometimes related to local disturbances such as the presence of replacement pegmatoid, potholes, or faulting, and in other cases resulting from less well-defined hydrothermal activity. In some areas, primary silicates have been replaced by low-temperature assemblages consisting of quartz, albite, sphene, and hydrous silicates (talc, prehnite, chlorite, epidote, and pumpellyite). In these areas, the base-metal sulphide assemblage consists of millerite + pyrite + chalcopyrite, instead of the pentlandite + chalcopyrite + pyrrhotite ± pyrite assemblage found in normal UG2. Such changes can be attributed to iron and sulphur loss resulting from sulphide–chromite equilibration and interaction with fluids. Expulsion of platinum-group elements (PGE) from base-metal sulphides during cooling resulted in the presence of platinum-group minerals, predominantly PGE-sulphides, enclosed in, or at the grain edges of, base-metal sulphides. Corrosion of sulphides by fluids leads to the isolation of these platinum-group minerals in hydrous silicates. Elsewhere, interaction with iron-rich metasomatic fluids resulted in a platinum-group mineral assemblage characterized by the presence of abundant Pt–Fe alloys, PGE sulpharsenides, PGE-bismuthtellurides, and other non-sulphide phases.

Introduction

The Bushveld Complex, outcrop and sub-outcrop of approximately 66 000 km^2 (Von Gruenewaldt, 1977), is the largest known layered intrusion. The uppermost chromitite layers in the Critical Zone, of which the UG2 is extensively mined for its platinum-group element (PGE) content, are renowned for their lateral persistency and consistency (Von Gruenewaldt *et al.*, 1986; Hatton and Von Gruenewaldt, 1987). Closer inspection, however, reveals considerable differences in the details of the UG2 Chromitite layer. These differences pertain to the thickness of the layer (McLaren and De Villiers, 1982; Gain, 1985; Shuttleworth, 1985a; 1985b; Von Gruenewaldt *et al.*, 1990), chromite composition (McLaren and De Villiers, 1982), the vertical distribution of PGE (McLaren and De Villiers, 1982; Gain, 1985; Mossom, 1986; Viljoen *et al.*, 1986a; 1986b; Von Gruenewaldt *et al.*, 1990), the grade and relative proportions of PGE (McLaren and De Villiers, 1982; Gain, 1985; Shuttleworth, 1985a; 1985b), the mineralogy of base-metal sulphides and platinum-group minerals (McLaren and De Villiers, 1982; Kinloch, 1982; Peyerl, 1982; Von Gruenewaldt *et al.*, 1990; Grimbeek, 1995), as well as the degree and style of alteration by late- to post-magmatic processes (Merkle, 1988; Winkels-Herding *et al.*, 1991; Grimbeek, 1995).

Some of these lateral variations result from processes operating on millimetre scale (Winkels-Herding *et al.*, 1991), others reflect continuous changes over short distances (Gain, 1985; Davey, 1992). Such variations may be due to local disturbances such as cross-cutting pipes (McLaren and De Villiers, 1982; Peyerl, 1982), or reflect regional differences (Von Gruenewaldt *et al.*, 1986; Bristow and Wilson, 1989; Lea, 1996).

In the western lobe of the Bushveld Complex, the Rustenburg Layered Suite can be divided into a northern and southern sector, separated by the Pilanesberg Alkaline Complex. The UG2 Chromitite layer in the southern part of the western Bushveld Complex is characterized by higher Pt:Pd and Pt:Rh ratios, while the *in situ* grade (over a typically thicker UG2) is lower than in other sectors (McLaren and De Villiers, 1982) (Figure 1). This thickness–grade relationship can be explained as the effect of two or more magma-mixing and ore-forming events which, through Rayleigh fractionation of

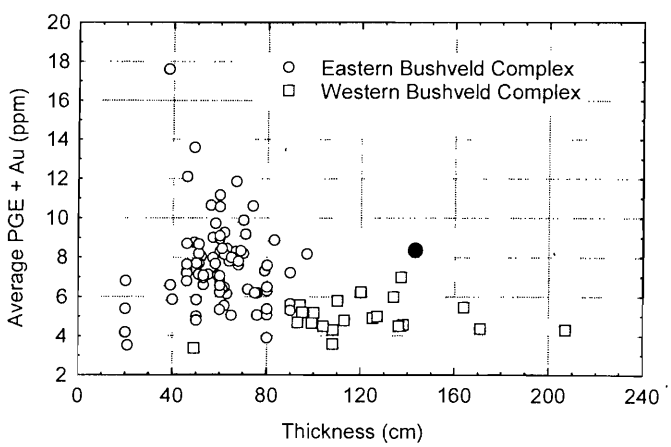

Figure 1 Relationship between the average grade of PGE + Au and thickness (Gain, 1985; Hiemstra, 1985; Shuttleworth, 1985a; 1985c; Von Gruenewaldt *et al.*, 1990; Grimbeek, 1995). The UG2 in the eastern Bushveld Complex generally has a higher grade over a smaller thickness than in the western Bushveld Complex. The solid black point represents atypically sulphur-rich UG2 from the eastern Bushveld Complex (Von Gruenewaldt *et al.*, 1990).

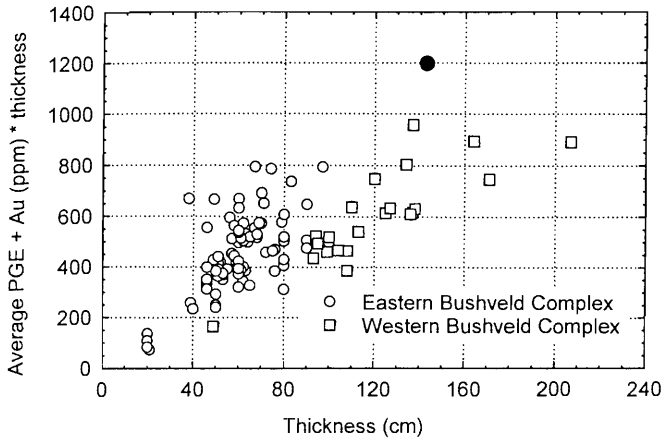

Figure 2 Relationship between the amount of PGE + Au in the UG2 Chromitite layer [expressed as average grade of (PGE + Au) * thickness] and the thickness of the layer. Although the concentration of PGE + Au decreases strongly with height in the UG2, and in this way decreases the average grade (Figure 1), the total amount of PGE + Au that can be beneficiated still tends to be higher in the western Bushveld Complex. The solid black point represents atypically sulphur-rich UG2 (Von Gruenewaldt *et al.*, 1990).

the PGE (Hiemstra, 1985; 1986), produce the typical pattern of grade distribution of two sharp peaks followed by decreasing PGE values with height through the UG2 layer. Deviations from this idealized pattern can be attributed to the combined effects of several different processes. Erosion of the lowermost, richest part of the UG2 by underlying pegmatoid (Hiemstra, 1985) may be the reason for an apparently missing bottom peak. Redistribution of PGE by late to post-magmatic fluids (Winkels-Herding *et al.*, 1991; Grimbeek, 1995) is another possible explanation.

The position of the upper peak in PGE concentration can, at least qualitatively, be related to the thickness of the layer. Again, too few detailed profiles of PGE distributions through the UG2 have been published (McLaren and De Villiers, 1982; Gain, 1985; Hiemstra, 1986) to evaluate this aspect on a statistically sound basis. It seems, however, that the upper peak of PGE concentration is at the top of the UG2 layer only if the thickness is low. Addition of more chromite at the top of the UG2 (*i.e.* if the pyroxenite partings which separate the chromitite stringers in the hanging-wall from the UG2 proper are missing) leads not only to an overall increase in the thickness of the UG2, but also causes the upper peak to apparently move to the middle portion of the layer (Davey, 1992). The addition of chromitite with lower PGE contents increases the thickness of the UG2 layer, while diluting the average grade (Figure 1). However, this additional chromite may still contain PGE in the parts per million range, which contributes to an overall higher absolute amount of potentially recoverable PGE (Figure 2).

The mineralogy of the PGE and the relative proportions of different platinum-group minerals in the UG2 also change along strike (Kinloch, 1982; McLaren and De Villiers, 1982; Peyerl, 1982; Mossom, 1986; Viljoen and Hieber, 1986; Viljoen *et al.*, 1986a; 1986b). Kinloch (1982) pointed out regional differences in platinum-group mineral assemblages, and the overall similarities in these assemblages in the Merensky Reef and the UG2 at different localities. Many of these variations can be ascribed to the effects of local disturbances like potholes or pegmatoids (Peyerl, 1982; Kinloch and Peyerl, 1990; Grimbeek, 1995).

Graben structures and intensive faulting between Brits and Kafferskraal caused extensive block faulting, making the UG2 more accessible to circulating fluids. This may explain the occurrence of millerite instead of pentlandite as the main nickel-carrying base-metal sulphide (McLaren and De Villiers, 1982; Verryn and Merkle, 1994) at some localities in this area.

An understanding of the reasons for mineralogical changes and their evaluation is important for successful beneficiation of UG2 ore. Textural differences, grain-size distributions, and relative proportions of platinum-group minerals impact on the recovery of PGE (Hofmeyr and Adair, 1993; Penberthy, 1996). Here we report on the results of an investigation to characterize different types of UG2 Chromitite from the Brits–Marikana area (western Bushveld Complex), ultimately relating variations in mineralogy with the behaviour of the ore during recovery. This paper, however, will only deal with the geological aspects of the research.

Sampling

Fourteen channel samples of UG2 Chromitite, covering the whole thickness of the layer, were collected underground from three different mining areas, labelled A, B, and C, in the Brits–Marikana district. Unfortunately, exact sample locations cannot be disclosed for reasons of confidentiality.

The samples originated from a range of geological environments and included:

- Samples of UG2 Chromitite with norite (sample numbers B2 and C2) and anorthosite footwall (sample numbers A2 and C5);
- Three samples of UG2 Chromitite with pegmatoid footwall (sample numbers A1, B1, and C4);
- Two samples associated with Fe-rich replacement pegmatoid (sample numbers A4 and B4);
- Three samples taken at the edge of pothole structures (sample numbers A3, B3, and C1). It should be noted that the area from which sample B3 was taken was possibly also affected by replacement pegmatoid activity;
- Three samples from fault zones (sample numbers A5, B4, and C2). Sample B4 was taken from an area affected by replacement pegmatoid activity.

Analytical techniques

Each sample was crushed to <2 mm and then split using a rotary sample riffler to provide a representative sample for mineralogical characterization. The samples were investigated using a range of mineralogical techniques, including optical microscopy (reflected and transmitted light), X-ray diffraction, electron-microprobe analysis, and scanning electron microscopy combined with image analysis and energy-dispersive X-ray analysis (EDX) (Penberthy, 1996). Grain-size distributions were based on area measurements on polished sections and the grain size expressed as equivalent circle diameter (ECD), that is the diameter of a circle with the same area as that of the measured grain ($ECD = 2 \times \sqrt{Area/\pi}$).

Results

Chromite

The UG2 Chromitite generally consists of subhedral chromite grains (about 65 mass per cent) in a silicate matrix comprising predominantly orthopyroxene and plagioclase. Textural features of chromite in the samples investigated are similar to those described by Hiemstra (1985), Hulbert and Von Gruenewaldt (1985), and Eales and Reynolds (1986), ranging from scattered chromite octahedra in a silicate matrix, to areas where large polygonal chromite grains form patches of densified chromitite, possibly as a result of sintering.

Chromite grain-size measurements (Figure 3) indicate that the median measured chromite diameters for most samples range between 164 and 177 μm. Chromite in the two samples associated with replacement pegmatoid are clearly coarser, with median chromite diameters of 221 μm for both samples. Similarly, an increase in chromite grain size was observed in the three samples taken at the edge of pothole structures, albeit to a lesser extent, with median grain diameters ranging from 184 to 191 μm.

Although some fracturing of chromite grains was observed in all three samples taken from fault zones, only one of these samples (A5) displays extensive cataclasis (Figure 4). The median chromite diameter in this sample is 127 μm.

Silicate mineralogy

Great variabilility is displayed in the silicate mineralogy, both between and within samples. In general, plagioclase ($\sim An_{88}$) is the most commonly found silicate phase, followed by orthopyroxene ($\sim En_{86}$). In areas of the samples where plagioclase is the dominant silicate, chromite grains may be separated from plagioclase by a thin rind of orthopyroxene. Similarly, orthopyroxene grains are sometimes separated from chromite by a plagioclase rim. Such textures have been interpreted by Eales and Reynolds (1986) as the products of reactions involving oxide, orthopyroxene, feldspar, and liquid. Most samples of UG2 Chromitite display some degree of alteration of orthopyroxene (and less commonly clinopyroxene) to talc, usually along grain boundaries and cleavage planes. Chloritization of plagioclase occurs locally.

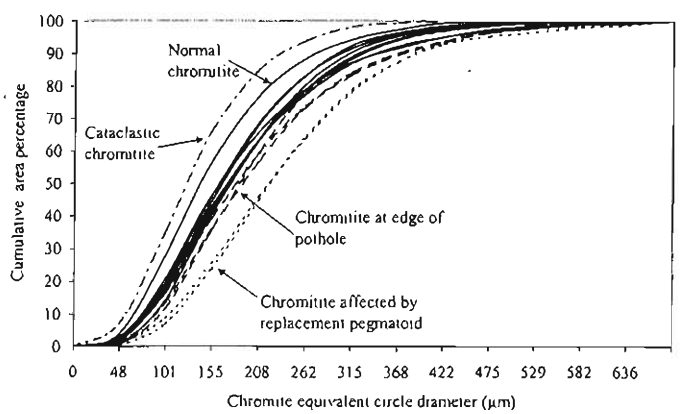

Figure 3 Cumulative chromite grain-size distributions of 14 samples based on area measurements on polished sections. Median equivalent circle diameter values for each sample can be read off along the X-axis where the 50% line indicated on the graph intersects the size distribution curve for that sample. Slight bin size inequalities are an artefact of the measuring technique.

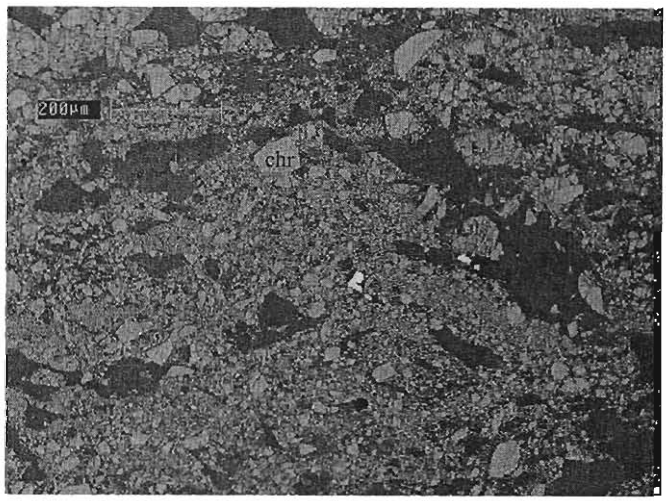

Figure 4 Cataclastic chromite (chr) cemented by chlorite, prehnite, and quartz (dark phases). Note the presence of pentlandite grains (brightest phase) in the silicate matrix. (Backscattered-electron image.)

Subsidiary amounts of intercumulus diopsidic clinopyroxene are present in most samples. A notable increase in clinopyroxene was observed in some sintered or densified areas, often displaying a similar type of texture to that described for plagioclase and orthopyroxene. In this case though, embayed grains of clinopyroxene and plagioclase are separated from chromite by a thin layer of pargasitic hornblende (Figure 5). Tremolite + talc and tremolite + chlorite assemblages, formed from clinopyroxene, were observed in a few areas.

Phlogopite (generally chlorine-bearing) is present in small amounts in all samples, representing a late magmatic phase, filling interstices between chromite and orthopyroxene or plagioclase grains. Trace amounts of a variety of late to post-

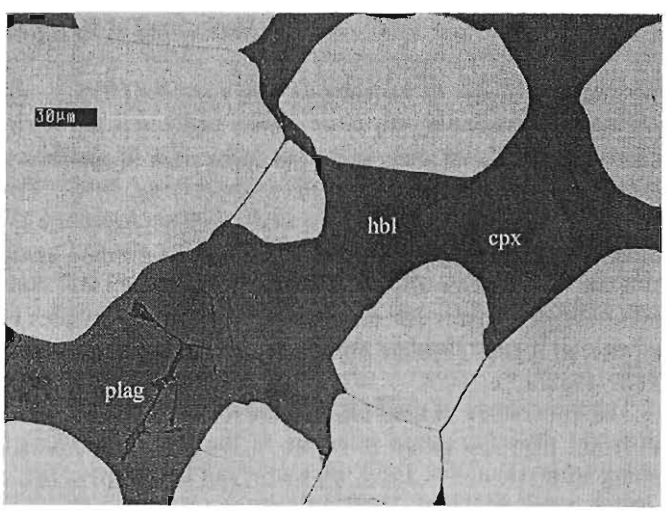

Figure 5 Embayed plagioclase (plag) and clinopyroxene (cpx) grains rimmed by pargasitic hornblende (hbl) Note the presence of chlorite veinlets (black) in plagioclase. (Backscattered-electron image)

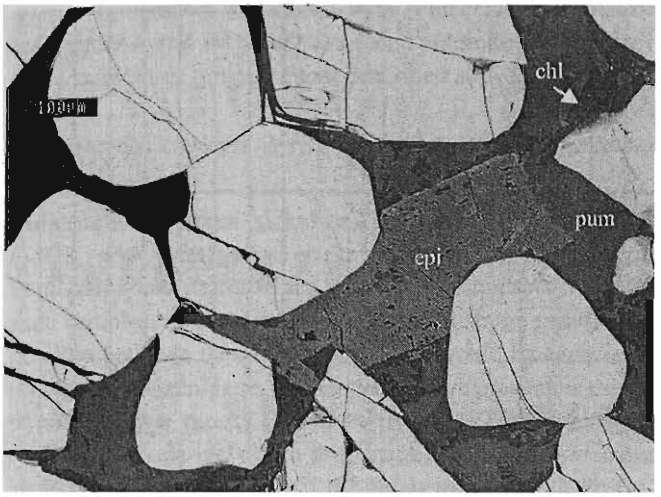

Figure 6 Euhedral epidote (epi) crystal in a matrix of pumpellyite (pum) edged by chlorite (chl). (Backscattered-electron image.)

magmatic phases can be found, including base-metal sulphides, platinum-group minerals, talc, chlorite (often chlorine-bearing), rutile, baddeleyite, sphene, chlorapatite, zircon, rare-earth element oxides, an unidentified Zr–Ti phase which is possibly srilankite (Merkle, 1992), epidote, prehnite, tremolite, quartz, albite, pumpellyite, and calcite associated with phlogopite.

Samples C1 to C5 are characterized by the replacement of the primary silicates by complex assemblages containing albite, quartz, pumpellyite, epidote, chlorite, talc, and less commonly, sphene, tremolite, prehnite, K-feldspar, calcite, and sericite (Figure 6). The extent of alteration ranges from isolated pockets to almost complete replacement of orthopyroxene and plagioclase in some samples. Although the alteration of silicate minerals could not be directly related to any specific geological disturbance (such as a fault or a pothole), the samples displaying the highest degree of alteration have abundant hydrothermal veins containing minerals such as calcite, quartz, prehnite, and chlorite. Since these samples were all taken in the same vicinity, it is likely that processes operating on a larger scale determined the mineralogical characteristics of the chromitite layer in this area, rather than local features such as pothole structures.

In cataclastic chromitite, fractured chromite grains are cemented by a number of secondary phases, including septechlorites, serpentine, quartz, pumpellyite, prehnite, chlorite, calcite, tremolite, and albite (Figure 4).

Base-metal sulphide mineralogy

The base-metal sulphide mineralogy of the samples investigated is summarized in Table 1. The samples were grouped together based on the geological environment from which they originated. However, because samples C1 to C5 are so obviously different from the other samples in terms of the mineralogy of the silicate minerals, and, as will be seen below, that of the base-metal sulphides and platinum-group minerals, it was decided to group these five samples separately.

Sulphur contents of the samples are low, ranging from 0.01 to 0.08 wt.%, with samples C1 to C5 characterized by low concentrations of sulphur (0.01 wt.%).

Normal UG2 (Sample numbers A1, A2, B1, B2)

The base-metal sulphide mineralogy of these samples is similar to that described for normal UG2 Chromitite by Grimbeek (1995) and McLaren and De Villiers (1982). The major base-metal sulphide minerals in samples of normal UG2 Chromitite are pentlandite (48 – 52 vol.%), chalcopyrite (24 – 29 vol.%), and pyrrhotite (4 – 29 vol.%). These minerals form composite grains at chromite–silicate grain boundaries, commonly in association with phlogopite and trace amounts of other hydrous silicates. Pyrite occurs as a minor constituent (1 – 16 vol.%), usually as chains of small grains in pentlandite. Subsidiary amounts of millerite (less than 5 vol.%) were observed in some of these samples, possibly replacing pentlandite. Rare grains of galena, usually smaller than 10 μm, occur in association with secondary hydrous silicates. A few isolated grains of Cu-rich sulphides (probably mostly bornite) were observed as inclusions in chromite.

Pyrrhotite sometimes appears to be partially rimmed by pentlandite and occasionally chalcopyrite. Similar textures from the Merensky Reef have been interpreted as resulting from magmatic fractionation (Kingston, 1966; Vermaak and Hendriks, 1976; Mostert *et al.*, 1982; Ballhaus and Stumpfl, 1986). Slight fraying of sulphide grain edges can sometimes be seen where they are in contact with secondary silicates. The median diameter of the sulphide composite grains ranges between approximately 30 and 32 μm, with a maximum of about 200 μm.

UG2 Chromitite associated with potholes and replacement pegmatoids

Except for slightly coarser sulphide grain sizes (median measured sulphide grain diameters are 33 to 39 μm in samples associated with potholes (samples A3 and B3), and 38 to

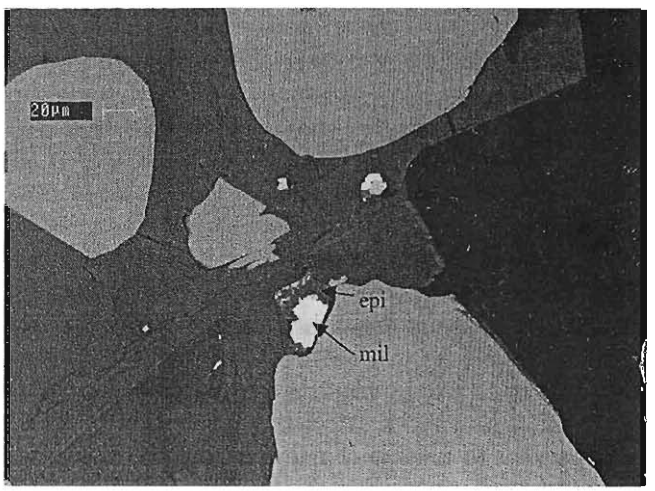

Figure 7 Corroded base-metal sulphide grain (BMS) (chalcopyrite + millerite + pyrite) with zoned braggite (brag) occurring at the grain boundary of chromite and orthopyroxene. Note the alteration of orthopyroxene (opx) to talc and the sulphide remnants in the talc rim around the sulphide grain. (Backscattered-electron image.)

Table 1 Relative amounts of base-metal sulphide (vol.%) in samples from different geological environments

	Anorthosite footwall	Norite footwall	Pegmatoid footwall		Pothole edge		Replacement pegmatoid footwall		Faulted UG2	Pothole edge	Norite footwall	Faulted UG2	Pegmatoid footwall	Anorthosite footwall
Sample no.	A2	B2	A1	B1	A3	B3	A4	B4	A5	C1	C2	C3	C4	C5
Chalcopyrite	27±4	29±6	24±4	25±5	28±8	19±5	26±10	15±1	23±8	43±9	32±15	54±13	34±10	49±6
Pentlandite	52±3	48±6	49±4	45±4	46±7	55±9	51±8	46±7	71±8	2±1	5±3	5±2	5±5	5±6
Pyrrhotite	13±4	4±2	19±3	29±7	14±4	25±5	22±5	35±7	6±4	--	1±1	2±3	5±5	0±2
Pyrite	8±1	16±5	8±1	1±1	11±6	1±1	1±0	3±2	--	11±8	31±13	15±16	16±4	20±5
Millerite	--	2±1	--	--	--	--	--	--	--	43±6	32±7	24±10	41±9	26±1
ECD (μm)	32	30	32	30	39	33	45	38	17	19	21	22	22	17
S (%)	0.02	0.01	0.03	0.05	0.04	0.03	0.05	0.08	0.02	0.01	0.01	0.01	0.01	0.01

ECD = median equivalent circle diameter of sulphide calculated from area measurements on polished sections. Statistical variation of S concentration levels is ±0.01% absolute (95% confidence level)

Table 2 Relative proportions of platinum group minerals expressed as vol. %

	Anorthosite footwall	Norite footwall	Pegmatoid footwall		Pothole edge		Replacement pegmatoid footwall		Faulted UG2	Pothole edge	Norite footwall	Faulted UG2	Pegmatoid footwall	Anorthosite footwall
Sample no.	A2 n=543	B2 n=471	A1 n=1766	B1 n=426	A3 n=433	B3 n=420	A4 n=420	B4 n=437	A5 n=425	C1 n=441	C2 n=445	C3 n=400	C4 n=425	C5 n=385
Pt–Pd–Ni–S	21±7	38±10	36±6	20±5	17±9	26±7	2±1	7±6	14±5	39±7	33±12	37±8	36±11	38±11
Pt–S	26±8	8±3	19±5	20±5	26±7	15±4	5±2	6±3	1±1	2±1	4±2	3±2	3±2	7±6
Pt–Rh–Ir–Cu–S	24±5	28±8	18±4	10±3	27±7	13±5	4±3	2±1	11±5	33±7	42±15	35±9	40±9	29±7
Ru–Os–Ir–S	23±6	17±6	19±4	27±7	22±6	29±7	31±8	33±8	30±9	22±7	16±6	20±9	18±5	23±8
PGE–Bi–Te	1±0	0±0	2±1	3±1	1±1	3±2	4±2	3±1	3±1	0±0	1±2	0±0	0±0	1±1
PGE–As–S	2±1	6±7	3±2	5±4	2±1	2±1	1±1	2±3	9±5	2±1	2±1	2±1	1±1	1±1
Pt–Fe alloy	2±1	0±0	2±1	9±4	5±4	10±4	40±8	45±9	17±9	0±0	0±0	0±0	0±0	0±0
Others	1±1	2±1	2±1	7±2	1±1	3±2	14±5	2±2	17±5	2±1	2±1	3±1	2±1	2±2

Statistical uncertainty, determined at the 95% confidence level, is reported as absolute variation; n is the number of platinum group mineral grains analysed

Table 3 Mode of occurrence of platinum-group minerals in fourteen samples of UG2 Chromitite reported in vol.%

	Anorthosite footwall	Norite footwall	Pegmatoid footwall		Pothole edge		Replacement pegmatoid footwall		Faulted UG2	Pothole edge	Norite footwall	Faulted UG2	Pegmatoid footwall	Anorthosite footwall
Sample no.	A2 n=334	B2 n=257	A1 n=665	B1 n=228	A3 n=184	B3 n=214	A4 n=199	B4 n=199	A5 n=196	C1 n=179	C2 n=205	C3 n=189	C4 n=207	C5 n=192
Liberated PGM	13±7	11±9	7±6	11±6	10±7	1±1	1±1	- -	- -	9±10	3±3	14±13	19±16	- -
Locked in BMS	23±8	24±8	26±9	32±8	27±14	26±8	27±8	40±19	7±4	7±4	8±5	0±0	12±8	6±4
Locked in chromite	7±4	4±3	2±1	9±10	3±2	12±9	12±10	6±5	8±5	2±2	4±3	6±3	5±3	7±4
Locked in silicate	6±3	10±10	2±1	10±5	12±5	5±2	10±6	12±6	44±9	42±11	40±17	29±11	34±10	44±12
BMS/Gangue	44±10	42±14	57±10	30±8	31±10	53±10	40±10	30±12	25±9	20±8	37±21	25±12	16±8	19±7
Chromite/Silicate	7±4	10±8	6±5	8±4	17±8	4±2	10±6	11±6	16±5	20±9	8±5	26±10	15±7	23±8
ECD (μm)	6	8	7	4	5	4	4	6	3	6	10	9	8	5

n = the number of platinum-group mineral grains investigated in the sample. Satistical uncertainty, determined at the 95% confidence level. is reported as absolute variation. Note that the differences in median platinum-group mineral grain size. expressed as ECD (equivalent circle diameter), between samples, are not statistically significant. PGM = platinum group metal; BMS = base-metal sulphide; / = grain boundary

49 μm in samples associated with replacement pegmatoids (samples A4 and B4), the base-metal sulphide mineralogy in these samples is similar to that described above.

Millerite–chalcopyrite–pyrite assemblages (sample numbers C1 to C5)

Millerite is the major nickel-bearing sulphide in samples C1 to C5, with pentlandite occurring in subsidiary amounts. Pentlandite and millerite are rarely found in direct contact in such samples, making it difficult to establish the genetic relationship between these two phases. As would be expected in this type of assemblage, pentlandite, where present, is usually of a nickel-rich variety (Misra and Fleet, 1973). Chalcopyrite constitutes a relatively high proportion of the sulphide minerals in these samples. Pyrite is the major iron-sulphide present, occurring both in composite grains with millerite and chalcopyrite, or as relatively coarse-grained porous pyrite at chromite–silicate grain boundaries or filling cracks in chromite. Siegenite [$(Co,Ni)_3S_4$] is a ubiquitous but minor component, usually associated with millerite.

In patches where primary silicate minerals persist, composite sulphide grains occur at chromite–silicate grain boundaries, usually associated with phlogopite and a host of secondary hydrous silicate minerals. Sulphide grains often display corroded outlines, appearing to have been partly replaced by secondary hydrous silicates (Figures 7, 8 and 9). This leads to a reduction in sulphide grain size (median measured grain diameters range from 17 to 22 μm in these samples) and lower concentrations of sulphide minerals (also reflected by low sulphur contents). More extensive alteration of primary silicate assemblages leads to local redistribution (probably on a scale of tens or hundreds of microns) and recrystallization of sulphide minerals, resulting in euhedral to subhedral sulphide grains intergrown with secondary silicates.

Base-metal sulphide assemblages with millerite as the major nickel-sulphide have also been described by McLaren (1980), Peyerl (1982), Winkels-Herding *et al.* (1991), and Verryn and Merkle (1994).

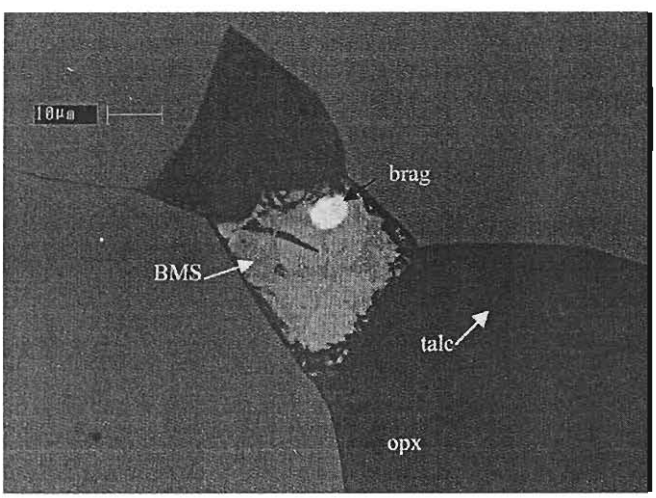

Figure 8 Corroded millerite (mil) grain rimmed by epidote (epi). Other phases are chromite, phlogopite, albite, pumpellyite, plagioclase, sphene, and pyrite. Note the presence of millerite remnants in epidote. (Backscattered-electron image).

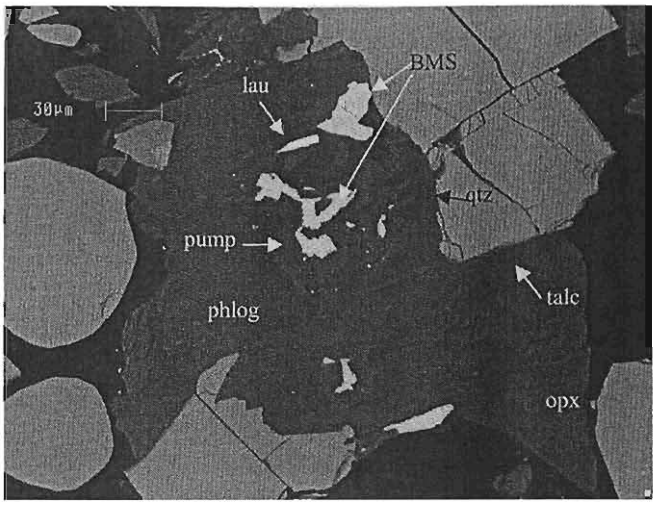

Figure 9 Recrystallized base-metal sulphides (chalcopyrite and millerite) (BMS) intergrown with pumpellyite (pum) and quartz (qtz), surrounded by phlogopite (phl). Note the presence of laurite (lau), originally in base-metal sulphide, isolated in silicate. Other phases present are chromite and orthopyroxene (opx) being replaced by talc. (Backscattered-electron image.)

Cataclastic UG2 Chromitite (sample number A5)

Pentlandite, chalcopyrite, and subsidiary pyrrhotite represent the base-metal sulphide assemblage in cataclastic UG2 chromite. Sulphide minerals generally occur in the silicate matrix cementing chromite grains. Relatively coarse, euhedral pentlandite grains were observed in places, suggesting recrystallization.

Platinum-group element mineralogy

The PGE contents of the samples investigated ranged between 3.17 and 5.87 ppm (Pt+Pd+Rh+Au). These elements are known to occur in the UG2 Chromitite layer, both as discrete platinum-group mineral grains (McLaren and De Villiers, 1982; Peyerl, 1982; Hofmeyr and Adair, 1993; Winkels-Herding *et al.*, 1991; Grimbeek, 1995) and submicroscopically, possibly in solid solution, in other minerals, notably Pd, Rh, and Ru in pentlandite (Paktunc *et al.*, 1990).

During the course of this study, more than 25 chemically distinct platinum-group mineral phases were observed. Platinum-group mineral phases were classified according to the presence of major elements, which were identified using qualitative EDX analysis. Due to resolution limitations during analysis of small platinum-group mineral grains included in base-metal sulphides, the presence of nickel, copper, cobalt and iron could not always be established in these phases. Quantitative electron-microprobe analysis of selected grains were used to confirm the identities of the most commonly occurring phases. For practical purposes these phases can be grouped together in the following eight categories (Table 2):

- Pt–Pd–Ni-sulphide (braggite and less commonly vysotskite);
- Pt–S (probably mostly cooperite);

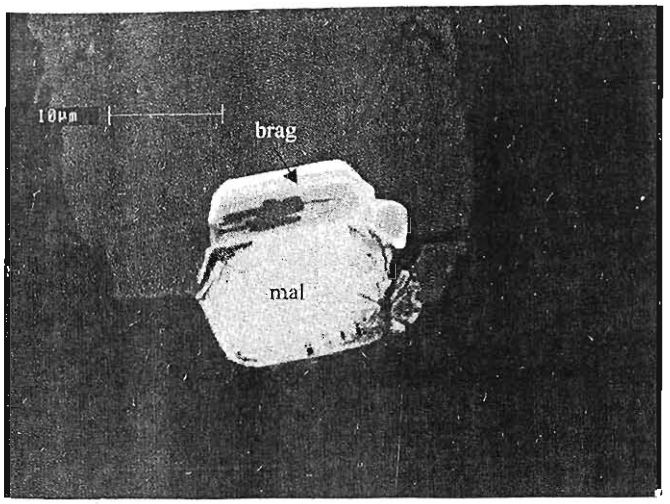

Figure 10 Zoned Pt–Pd–Ni-sulphide grain (brag) (more platinum-rich towards the rim) attached to Pt–Rh–Ir–Cu-sulphide (mal). Note the skeletal appearance of Pt–Rh–Ir–Cu-sulphide at the grain edge. The associated sulphides are pentlandite and chalcopyrite. (Back-scattered-electron image.)

- Pt–Rh–Ir–Cu–S (probably malanite, usually cobalt-bearing);
- Ru–Os–Ir–S (laurite–erlichmanite);
- PGE–Bi–Te (various tellurides, bismuthides, and bismuthtellurides of platinum and palladium);
- PGE–As–S (includes a variety of sulpharsenides and arsenides such as hollingworthite, irarsite, ruarsite, sperrylite, and majakite);
- Pt–Fe (alloys of platinum and iron, often contain palladium and rhodium, sometimes copper); and
- Others (a host of minerals, usually palladium-bearing, consisting of various compounds of PGE with Hg, Pb, Ge, Sb, As, Bi, Te, and Sn)

All platinum-group mineral grains observed were also classified according to their textural setting into one of the following categories (Table 3):

- Liberated platinum-group minerals, that is grains that were freed from the rock matrix during crushing. Most of these grains were probably located at grain boundaries prior to crushing;
- Locked in base-metal sulphide, refers to platinum-group mineral grains enclosed in base-metal sulphide composite grains, including platinum-group mineral grains at sulphide–sulphide grain boundaries;
- Locked in chromite, refers to platinum-group mineral grains enclosed in chromite;
- Locked in silicate, includes platinum-group mineral grains occurring both as inclusions in silicate and at silicate–silicate grain boundaries;
- Platinum-group mineral grains occurring at the grain boundaries of base-metal sulphides with silicate and/or chromite; and
- Platinum-group mineral grains occurring at the grain boundaries of chromite and silicate.

Significant differences could be seen between samples, in terms of both modal proportions (Table 2) and mode of occurrence (Table 3).

Normal UG2 Chromitite (sample numbers A1, A2, B1, B2)

Most of the platinum-group minerals (more than 60 vol.%) occur associated with base-metal sulphides, either at the grain boundaries of sulphide with chromite or silicate, or enclosed by base-metal sulphides, particularly pentlandite. The remainder of the platinum-group minerals occur at chromite–silicate, or silicate–silicate grain boundaries, locked in chromite (less than 10 vol.%, usually laurite–erlichmanite), or within silicate minerals. Platinum-group mineral grain sizes range from <1 µm to approximately 30 µm, with a median value of approximately 6 µm (Table 3).

As documented by other authors (McLaren and De Villiers, 1982; Grimbeek, 1995), the platinum-group mineral assemblages in normal UG2 samples consist predominantly (more than 90 vol.%) of sulphides, predominantly Pt–Pd–Ni sulphide, Pt-sulphide, Pt–Rh–Ir–Cu-sulphide, and laurite, tending towards euhedral to subhedral forms. Pt–Pd–Ni-sulphide grains are often zoned, displaying in their simplest form a palladium-rich core surrounded by a platinum-rich rim (Figure 10). Cousins and Kinloch (1976) speculated that during weathering, nickel and palladium are preferentially leached out of braggite, resulting in a phase with a chemical composition corresponding to that of cooperite, and with the structure and optical properties of braggite. It is suggested that a similar process, operating under post-magmatic conditions, may account for zoned Pt–Pd–Ni-sulphide grains in UG2 Chromitite.

Where Pt–Rh–Ir–Cu-sulphide occurs in pentlandite, it often appears to form skeletal grains. Low-temperature palladium-bearing phases such as Pd–Pb are occasionally present as tiny veinlets, of the order of 1 µm across, usually forming part of base-metal sulphide composite grains.

UG2 Chromitite associated with potholes and replacement pegmatoids

The platinum-group mineral assemblages in samples collected from the edge of pothole structures (samples A3 and B3) do not differ significantly from those of normal UG2 Chromitite. UG2 Chromitite associated with replacement pegmatoid, however, is characterized by platinum-group mineral assemblages consisting predominantly of Pt–Fe alloys (often rhodium- or palladium-bearing), laurite, and to a lesser extent PGE–Bi–Te compounds, and other non-sulphide platinum-group minerals. Similar changes in the platinum-group mineral assemblages of samples from such environments have been documented by a number of researchers (McLaren and De Villiers, 1982; Peyerl, 1982; Viljoen and Scoon, 1985; Grimbeek, 1995). Pt–Fe alloys often display emulsion intergrowth textures with base-metal sulphides (McLaren and De Villiers, 1982; Peyerl, 1982; Kinloch and Peyerl, 1990; Grimbeek, 1995) (Figure 11). The data do not, however, indicate any significant increase in platinum-group mineral grain size (Table 3), as documented by Peyerl (1982) and Grimbeek (1995), or any increase in the proportion of platinum-group minerals associated with silicates (Grimbeek, 1995).

Platinum-group minerals associated with millerite–pyrite–chalcopyrite assemblages (sample numbers C1 to C5)

One of the most striking aspects of the platinum-group minerals assemblages from the mining area represented by these

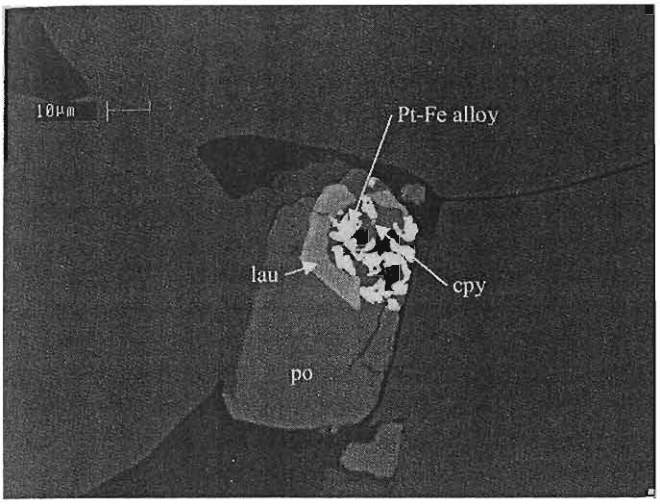

Figure 11 Backscattered-electron image showing an emulsion intergrowth of Pt–Fe alloy with chalcopyrite (cpy) occurring with pyrrhotite (po) at the grain boundary of silicate and chromite. This texture appears to be partly rimmed by a zoned laurite grain (lau). (The higher backscatter-electron intensity in the rim is a result of higher concentration levels of Os.)

samples, is the sharp drop in the modal proportions of Pt-sulphide and a concomitant increase in Pt–Rh–Ir–Cu-sulphide and Pt–Pd–Ni-sulphide, compared to normal UG2 Chromitite. These differences were tested and found to be significant at the 95% confidence level. Bulk chemical analyses do not show any accompanying changes in Pt/Rh and Pt/Pd ratios. Qualitative EDS analysis of Pt–Pd–Ni-sulphide also suggests a change to more palladian compositions. The evidently complete absence of Pt–Fe alloys in these samples is also significant.

A significantly lower proportion of the platinum-group minerals in these samples is associated with base-metal sulphides (25 – 45%). Most of the platinum-group minerals occur in contact with secondary hydrous silicates, often at silicate–silicate grain boundaries, usually in the vicinity of base-metal sulphides (Figure 9).

Cataclastic UG2 Chromitite (sample number A5)

The platinum-group element mineralogy in this sample is dominated by laurite and non-sulphide platinum-group minerals such as Pt–Fe alloys. Although Pt–Rh–Ir–Cu-sulphide and Pt–Pd–Ni-sulphides still represent a significant proportion of the platinum-group minerals, Pt-sulphide was rarely observed. The platinum-group minerals are predominantly associated with secondary hydrous silicates.

Discussion

Normal UG2 Chromitite

If it is assumed that the base-metal sulphides in the UG2 originally formed from an immiscible sulphide melt which underwent crystallization and exsolution of pentlandite and chalcopyrite in a pyrrhotite-dominated matrix (Kullerud *et al.*, 1969), then it is clear that the present mineral assemblage does not represent a primary magmatic sulphide assemblage. The present assemblage of pentlandite > pyrrhotite and chalcopyrite indicates a loss of iron and equilibration to low temperatures (Kullerud *et al.*, 1969; Ballhaus and Ryan, 1995; Ballhaus and Ulmer, 1995). Sulphide assemblages associated with the chromitite layers of the Bushveld Complex are enriched in PGE, nickel, and copper compared to typical magmatic sulphide assemblages (Von Gruenewaldt *et al.*, 1986; Naldrett and Lehmann, 1987). The high nickel and copper tenors of these sulphide assemblages are reflected by the dominance of pentlandite and chalcopyrite, and the relative paucity of pyrrhotite. Gain (1985) and Von Gruenewaldt *et al.* (1986) suggested that the original mass of these sulphides has been greatly reduced by the removal of iron and sulphur, with the consequent enrichment of other metals. Naldrett and Lehmann (1987) and Naldrett *et al.* (1989) demonstrated the feasibility of such a process, in which iron may be lost from magmatic sulphides to fill vacancies in non-stoichiometric chromite crystallizing from basaltic magma. Release of sulphur resulting from the dissociation of magmatic pyrrhotite may lead to the formation of pyrite from pyrrhotite. Once the most sulphur-rich assemblage possible under the prevailing conditions has formed, further extraction of iron will lead to a bulk loss of sulphur (Merkle, 1992).

The platinum-group minerals in typical UG2 Chromitite are predominantly sulphides of platinum and/or palladium (cooperite, braggite, and less commonly, vysotskite), Pt–Rh–Ir–Cu–S (probably malanite) and laurite, and are generally associated with base-metal sulphides, occurring either at sulphide grain boundaries with silicates or chromite, at sulphide–sulphide grain boundaries, or as inclusions in sulphide.

Experimental studies have shown that at elevated temperatures, the base-metal sulphides, especially pyrrhotite, pentlandite, and millerite, can accommodate significant amounts of PGE in solid solution (*e.g.* Distler *et al.*, 1977; Makovicky *et al.*, 1986; Karup-Møller and Makovicky, 1993; Ballhaus and Ulmer, 1995), most of which will be expelled on cooling to form discrete platinum-group minerals. Chalcopyrite appears to be barren of PGE, even at elevated temperatures. Calculations by Ballhaus and Ryan (1995) show that at temperatures as low as 500 °C, the entire PGE content of the Merensky Reef can be accommodated in solid solution in base-metal sulphides. This may not be the case for UG2 Chromitite, where PGE tenors are much higher. Ballhaus and Ryan (1995) and Ballhaus and Ulmer (1995) suggest that the association of discrete platinum-group minerals with base-metal sulphides reflect equilibration at temperatures as low as or below 100 °C.

In many places, pegmatoid forms the footwall to the UG2 (Hiemstra, 1985; Viljoen *et al.*, 1986b; Cawthorn and Barry, 1992; Davey, 1992; Van der Merwe *et al.*, 1998). Although the physical erosion of the lowermost part of the UG2 may be responsible for elevated PGE contents in the footwall, and also for an apparently missing bottom peak of PGE contents, this type of footwall does not seem to be associated with any significant change in the mineralogy of the UG2 itself. The overall very similar proportions of base-metal sulphides (Table 1) and platinum-group minerals (Table 2), compared to normal UG2 with non-pegmatoidal footwall, supports the view of Hiemstra (1985) that the formation of the pegmatoid post-dates the formation of the UG2 Chromitite.

UG2 Chromitite associated with replacement pegmatoid and potholes

UG2 Chromitite associated with replacement pegmatoid, and possibly potholes, are characterized by annealing of chromite grains accompanied by an increase in clinopyroxene, possibly of hydrothermal origin (Manning and Bird, 1986), and the formation of hornblende. Similar changes in silicate mineralogy were described by Merkle (1988) in UG1 Chromitite as a result of interaction with metasomatizing fluids.

The base-metal sulphide mineralogy from samples associated with iron-rich replacement pegmatoid (Viljoen and Scoon, 1985; Gain, 1985; Viljoen *et al.*, 1986a; 1986b; Leeb-du-Toit, 1986; Farquhar, 1986; Hofmeyr and Adair, 1993; Grimbeek, 1995; Van der Merwe *et al.*, 1998) is similar to that of normal UG2 Chromitite, aside from a slight increase in grain sizes. Other authors (McLaren and De Villiers, 1982; Peyerl, 1982; Grimbeek, 1995) have described more complex sulphide assemblages containing minerals such as chalcocite, bornite, violarite, mooihoekite, haycockite, digenite, native copper, cubanite, mackinawite, heazlewoodite, and millerite in samples affected by replacement pegmatoid and dunite pipes. These deviations in base-metal sulphide mineralogy can be attributed to variable degrees of metasomatic effects from the replacement pegmatoid.

Platinum-group mineral assemblages in such areas are dominated by laurite, Pt–Rh–Fe and Pt–Pd–Fe alloys, and other non-sulphide platinum-group minerals. The formation of such platinum-group mineral assemblages have been attributed to higher f_{O_2}, possibly as a result of increased volatile activity resulting in lower f_{S_2} (Peyerl, 1982; Kinloch, 1982; McLaren and De Villiers, 1982; Estigneeva *et al.*, 1995).

In the case of UG2 Chromitite associated with pothole structures, the platinum-group mineral assemblages are not sufficiently different from those of normal UG2 Chromitite to allow any conclusions. Merensky Reef pothole structures are believed to be areas of increased volatile activity (*e.g.* Campbell, 1986; Cawthorn and Poulton, 1988; Ballhaus, 1988; Kinloch, 1982; Kinloch and Peyerl, 1990; Boudreau, 1992) and several authors have suggested a genetic link between replacement pegmatoid and pothole structures (Viljoen and Hieber, 1986; Farquhar, 1986; Kinloch and Peyerl, 1990). Cawthorn and Barry (1992) found no evidence of fluid channeling through UG2 potholes. A discussion on the origin of pothole structures is beyond the scope of this investigation. However, from the limited data available, it is tentatively suggested that the possibility of increased fluid activity associated with UG2 potholes cannot be summarily dismissed.

Effects of low-temperature hydrothermal alteration (samples C1 – C5)

The replacement of primary silicates by mineral assemblages containing albite, quartz, pumpellyite, epidote, chlorite, prehnite, sphene, and talc is similar to that described by Schiffries and Skinner (1987) and Schiffries and Rye (1990), resulting from the interaction of hydrothermal fluids with wallrock at temperatures below about 600 °C.

Corrosion of base-metal sulphides by hydrothermal fluids leads, in places, to iron and sulphur loss, in addition to the losses as a result of sulphide–chromite equilibration (Merkle, 1992). This leads to the formation of low-temperature, high-f_{S_2} sulphide assemblages, consisting of chalcopyrite, millerite, pyrite, and subsidiary siegenite. Such assemblages could not have exsolved from a magmatic sulphide melt (Kullerud *et al.*, 1969; Craig and Kullerud, 1969). Based on the lack of mineral textures suggesting replacement of pentlandite by millerite, and phase relations in the Ni–Fe–S and Ni–S systems (Kullerud and Yund, 1962; Vaughan and Craig, 1978), Verryn and Merkle (1994) suggested that millerite formed directly from hydrothermal fluids at temperatures below 379 °C.

Platinum-group mineral assemblages in these areas are similar to those occurring in normal UG2, but with noticeably lower concentrations of platinum sulphide and a concomitant increase in malanite, braggite, and vysotskite, possibly indicating lower temperature of formation under conditions of higher f_{S_2} (Knacke *et al.*, 1991). The absence of Pt–Fe alloys also points to conditions of increased sulphur fugacity. Reduction of the volume of base-metal sulphides through loss of iron and sulphur, due to the interaction of base-metal sulphides with chromite and fluids, results in the platinum-group minerals (previously associated with base-metal sulphides) becoming isolated in hydrous silicates filling the spaces previously occupied by sulphides (Figure 9).

It is tentatively suggested that the relatively high modal proportions of palladium- and rhodium-bearing sulphides (Table 2), compared to platinum-group mineral assemblages from normal UG2, is a consequence of the paucity of pentlandite in these samples. It is known that pentlandite in UG2 and Merensky ore contains small amounts of palladium and rhodium in solid solution (Paktunc *et al.*, 1990; Ballhaus and Ryan, 1995). Hence, the scarcity of pentlandite may lead to a higher proportion of palladium- and rhodium-bearing platinum-group minerals.

Cataclasic UG2

The presence of fractures in faulted areas makes the UG2 Chromitite layer more accessible to circulating fluids. Interaction of these fluids with primary silicate minerals causes the formation of hydrous silicates, quartz, and calcite cementing fractured chromite grains. The platinum-group mineral assemblage is characterized by the presence of significant amounts of non-sulphide minerals such as Pt–Fe alloy and PGE sulpharsenides, which can be also attributed the effects of fluids at intermediate to low temperatures.

Summary and conclusions

Large variations in mineralogy, in terms of the modal proportions and compositions of minerals, as well as their textural settings, have been observed in the UG2 Chromitite layer over a relatively short distance (30 – 50 km). Most of these variations can be safely attributed to post-magmatic modification by fluids.

- The replacement of primary silicate assemblages in UG2 Chromitite (orthopyroxene, plagioclase, and minor phlogopite) by albite, quartz, pumpellyite, epidote, prehnite, chlorite, sphene, and talc in some samples suggests interaction with hydrothermal fluids at temperatures below 600 °C.

- Annealing of chromite grains and the formation of clinopyroxene and amphibole characterizes the silicate mineralogy of UG2 Chromitite in the vicinity of replacement pegmatoid, and can be attributed to the effects of iron-rich metasomatizing fluids.
- The base-metal sulphide assemblage in normal UG2 Chromitite consists of pentlandite, chalcopyrite, pyrrhotite, and minor pyrite. It is suggested that this assemblage is the result of post-magmatic iron and sulphur loss due to chromite–sulphide equilibration combined with fluid activity and does not represent a primary magmatic assemblage. Platinum-group minerals form by the expulsion of platinum-group elements from base-metal sulphides during cooling, explaining their close association with base-metal sulphides. In normal UG2 Chromitite, the platinum-group mineral assemblage consists predominantly of sulphides (cooperite, braggite, malanite, and laurite).
- Interaction of magmatic base-metal sulphides with hydrothermal fluids leads to corrosion of sulphides and the precipitation of sulphide-rich, low-temperature chalcopyrite–millerite–pyrite assemblages. The reduction of base-metal sulphide sizes in areas where millerite is the dominant nickel-bearing base-metal sulphide causes the isolation of platinum-group minerals from base-metal sulphides, as shown by the occurrence of platinum-group minerals in silicates and at chromite–silicate boundaries. Platinum-group mineral assemblages from these areas are characterized by a decrease in the relative amount of cooperite, and an increase in braggite and malanite, compared to normal UG2.
- Platinum-group mineral assemblages range from predominantly sulphide assemblages (cooperite, braggite, malanite, and laurite) in normal UG2 to assemblages dominated by laurite, Pt–Rh–Fe and Pt–Pd–Fe in UG2 Chromitite associated with replacement pegmatoid.
- Faulting causes cataclasis of chromitite in some areas. Fractures act as conduits for fluids, leading to the cementation of fractured chromite grains by low-temperature hydrous silicates, quartz, and calcite. These conditions lead to the formation of non-sulphide platinum-group minerals enclosed in silicate.

These mineralogical variations can be sometimes related to local disturbances, such as the presence of replacement pegmatoid, potholes, or faulting, but in some cases appear to result from less well-defined hydrothermal activity.

Acknowledgements

Lonrho's Platinum Division is gratefully acknowledged for supplying the samples and permission to publish results. Many colleagues at Mintek, in particular Dr. E.J. Oosthuyzen, Mr. E.A. Viljoen, Ms. L.A. Andrews, Ms. J.C. Mostert, Dr. J.P.R. de Villiers, and Dr. J. Nell, as well as Prof. S.A. de Waal of the University of Pretoria also contributed to this investigation, for which we thank them. This paper is published by permission of Mintek.

References

Ballhaus, C.G. (1988). Potholes of the Merensky Reef at Brakspruit shaft, Rustenburg Platinum Mines; Primary disturbances in the magmatic stratigraphy. *Econ. Geol.*, **83**, 1140–1158.

Ballhaus, C.G. and Ryan, C.G. (1995). Platinum-group elements in the Merensky Reef. I. PGE in solid solution in base metal sulfides and the down-temperature equilibration history of Merensky ores. *Contr. Miner. Petrol.*, **122**, 241–251.

Ballhaus, C.G. and Stumpfl, E.F. (1986). Sulfide and platinum mineralization in the Merensky Reef: evidence from hydrous silicates and fluid inclusions. *Contr. Miner. Petrol.*, **94**, 193–204.

Ballhaus, C.G. and Ulmer, P. (1995). Platinum-group elements in the Merensky Reef: II. Experimental solubilities of platinum and palladium in Fe_{1-x} from 950 to 450 °C under controlled f_{S_2} and f_{H_2}. *Geochim. Cosmochim. Acta*, **59**, 4881–4888.

Boudreau, A.E. (1992). Volatile fluid overpressure in layered intrusions and the formation of potholes. *Aust. J. Earth Sci.*, **39**, 277–287.

Bristow, D.M. and Wilson, A.H. (1989). Lateral variations in the PGE bearing UG2 Chromitite as related to the discontinuity between the southern and central sectors of the eastern Bushveld Complex. *Bull. Geol. Soc. Finland*, **61**, 15.

Campbell, I.H. (1986). A fluid dynamic model for the potholes of the Merensky Reef. *Econ. Geol.*, **81**, 1118–1125.

Cawthorn, R.G. and Barry, S.D. (1992). The role of intercumulus residua in the formation of pegmatoid associated with the UG-2 Chromitite, Bushveld Complex. *Austr. J. Earth Sci.*, **39**, 263–276.

Cawthorn, R.G. and Poulton, K.L. (1988). Evidence for fluid in the footwall beneath potholes in the Merensky Reef of the Bushveld Complex. *In*: Prichard, H.M., Potts, P.J., Bowles, J.F.W. and Cribb, S.J. (Eds.), *Geoplatinum '87*, April 22–23, 1987, Elsevier Sci. Publ., Essex, Milton Keynes, 343–356.

Cousins, C.A. and Kinloch, E.D. (1976). Some observations on textures and inclusions in alluvial platinoids. *Econ. Geol.*, **71**, 1377–1395.

Craig, J.R. and Kullerud, G. (1969). Phase relations in the Cu–Fe–Ni–S system and their application to magmatic ore deposits. *In:* Wilson, H.D.B. (Ed.). *Magmatic Ore Deposits.* Monogr. Econ. Geol., **4**, 344–358.

Davey, S.R. (1992). Lateral variations within the upper Critical Zone of the Bushveld Complex on the farm Rooikoppies 297JQ, Marikana, South Africa. *S. Afr. J. Geol.*, **95**, 141–149.

Distler, V.V., Malevskiy, A.Y. and Laputina, I.P. (1977). Distribution of platinoids between pyrrhotite and pentlandite in crystallisation of a sulfide melt. Translated from *Geokhimiy*, **11**, 1646–1657.

Eales, H.V. and Reynolds, I. M. (1986). Cryptic variations within chromitites of the Upper Critical Zone, Northwestern Bushveld Complex. *Econ. Geol.*, **81**, 1056–1066.

Evstigneeva, T., Moh, G.H. and Tarkian, M. (1995). Hydrothermal recrystallization of PGE- and Fe–Ni-sulfide assemblages. *N. Jb. Miner. Abh.*, **169**, 273–277.

Farquhar, J. (1986). The Western Platinum Mine. *In*: Anhaeusser, C.R. and Maske, S. (Eds.), *Mineral Deposits of Southern Africa.* Geol. Soc. S. Afr., Johannesburg, S. Afr., **II**, 1135–1142.

Gain, S.B. (1985). The geologic setting of the platiniferous UG-2 Chromitite layer on the farm Maandagshoek, Eastern Bushveld Complex. *Econ. Geol.* **80**, 925–943.

Grimbeek, J.C. (1995). *The effect of the Vaalkop replacement pegmatoid on the sulphide mineralogy at Western Platinum Mine in the Mooinooi District.* M.Sc. thesis (unpubl.), Univ. Pretoria, S. Afr., 110 pp.

Hatton, C.J. and Von Gruenewaldt, G. (1987). The geological setting and petrogenesis of the Bushveld chromitite layers. *In*: Stowe, C.W. (Ed.), *Evolution of Chromium Ore Fields.* Van Norstrand Reinhold, Stroudsberg Pennsylvania, 109–143.

Hiemstra, S.A. (1985). The distribution of some platinum-group elements in the UG-2 Chromitite layer of the Bushveld Complex. *Econ. Geol.*, **80**, 944–957.

Hiemstra, S.A. (1986). The distribution of chalcophile and platinum-group elements in the UG-2 Chromitite layer of the Bushveld Complex. *Econ. Geol.*, **81**, 1080–1086.

Hofmeyr, P.K. and Adair, B.J.I. (1993). The effect on precious metal recovery of an unusual mineralogical regime within the Merensky Reef and UG-2 Chromitite layer at Rustenburg, South Africa. *In*: Griffin, B., Graham, J. and Linge, H. (Eds.), *Progm. Abstr. ICAM '93*, 22 May – 2 June, 1993, Freemantle, Western Australia, 209–212.

Hulbert, L.J. and Von Gruenewaldt, G. (1985). Textural and compositional features of chromite in the Lower and Critical Zones of the Bushveld Complex South of Potgietersrus. *Econ. Geol.*, **80**, 872–895.

Karøp-Moller, S. and Makovicky, E. (1993). The system Pd–Ni–S at 900 ° 725 °, 550 ° and 400 °C. *Econ. Geol.*, **88**, 1261–1268.

Kingston, G.A. (1966). The occurrence of platinoid bismuthotellurides in the Merensky Reef at Rustenburg platinum mine in the western Bushveld. *Mineral. Mag.*, **35**, 815–833.

Kinloch, E.D. (1982). Regional trends in the platinum-group mineralogy of the Critical Zone of the Bushveld Complex, South Africa. *Econ. Geol.*, 77, 1328–1347.

Kinloch, E.D. and Peyerl, W. (1990). Platinum-group minerals in various rock types of the Merensky Reef: Genetic implications. *Econ. Geol.*, **85**, 537–555.

Knacke, O., Kubaschewski, O. and Hesselmann, K. (Eds.) (1991). *Thermochemical Properties of Inorganic Substances*. Springer-Verlag, Berlin, Heidelberg, New York, 2142 pp.

Kullerud, G. and Yund, R.A. (1962). The Ni–S system and related minerals. *J. Petrol.*, **3**, 126–175.

Kullerud, G., Yund, R.A., and Moh, G.H. (1969). Phase relations in the Cu–Fe–S, Cu–Ni–S, and Fe–Ni–S systems. *In:* Wilson, H.D.B. (Ed.), *Magmatic Ore Deposits*. Monogr. Econ. Geol., **4**, 323–343.

Lea, S.D. (1996). The geology of the Upper Critical Zone, northeastern Bushveld Complex. *S. Afr. J. Geol.*, **99**, 263–283.

Leeb-Du Toit, A. (1986). The Impala Platinum Mines. *In*: Anhaeusser, C.R. and Maske, S. (Eds.), *Mineral Deposits of Southern Africa*. Geol. Soc. S. Afr., Johannesburg, **II**, 1091–1106.

Makovicky, M., Makovicky, E. and Rose-Hansen, J. (1986). Experimental studies on the solubility and distribution of platinum-group elements in base-metal sulphides in platinum deposits. *In*: Gallagher, M.J., Ixer, R.A., Neary, C.R. and Prichard, H.M. (Eds.), *Metallogeny of Basic and Ultrabasic rocks*. Inst. Min. Metall., 415–425.

Manning, C.E. and Bird, D.K. (1986). Hydrothermal clinopyroxenes of the Skaergard Intrusion. *Contrib. Mineral. Petrol.*, **92**, 437–447.

McLaren, C.H. (1980). *'n Mineralogiese ondersoek van die platinumgroepminerale in die boonste chromitietlaag (UG2) van die Bosveldkompleks*. Ph.D. thesis (unpubl.), Rand Afrikaans Univ., Johannesburg, S. Afr., 360 pp.

McLaren, C.H. and De Villiers, J.P.R. (1982). The platinum-group chemistry and mineralogy of the UG-2 Chromitite layer of the Bushveld Complex. *Econ. Geol.*, 77, 1348–1366.

Merkle, R.K.W. (1988). The effects of metasomatising fluids on the PGE-content of the UG-1 Chromitite layer. *In*: Prichard, H.M., Potts, P.J., Bowles, J.F.W. and Cribb, S.J. (Eds.), *Geoplatinum '87*. Elsevier Sci. Publ., Essex, Milton Keynes, UK, 359–360.

Merkle, R.K.W. (1992). Platinum-group minerals in the middle group of chromitite layers at Marikana, western Bushveld Complex: indications for collection mechanisms and postmagmatic modification. *Can. J. Earth Sci.*, **29**, 209–221.

Mossom, R.J. (1986). The Atok Platinum Mine. *In*: Anhaeusser, C.R. and Maske, S. (Eds.), *Mineral Deposits of Southern Africa*. Geol. Soc. S. Afr., Johannesburg, S. Afr., **II**, 1143–1154.

Mostert, A.B., Hofmeyr, P.K. and Potgieter, G.A. (1982). The platinum-group mineralogy of the Merensky Reef at the Impala Platinum Mines, Bophutatswana. *Econ. Geol.*, 7, 1385–1394.

Misra, K.C. and Fleet, M.E. (1973). The chemical compositions of synthetic and natural pentlandite assemblages. *Econ. Geol.*, **68**, 518–539.

Naldrett, A.J.and Lehmann, J. (1987). Spinel non-stoichiometry as the explanation for Ni-, Cu-, and PGE-enriched sulphides in chromitites. *In:* Prichard, H.M., Potts, P.J., Bowles, J.F.W. and Cribb, S.J. (Eds.), *Geoplatinum '87*. Elsevier, Amsterdam, The Netherlands, 93–109.

Naldrett, A.J., Lehmann, J. and Augé, T. (1989). Spinel non-stoichiometry and reactions between chromite and closely associated sulphides, with examples from ophiolite complexes. *In*: Prendergast, M.D. and Jones, J. (Eds.), *Magmatic Sulphides — the Zimbabwe Volume*. Inst. Min. Metall., London, UK, 221–227.

Paktunc, A.D., Hulbert, L.J. and Harris, D.C. (1990). Partitioning of the platinum-group and other trace elements in sulfides from the Bushveld Complex and Canadian occurrences of nickel–copper sulfides. *Can. Miner.*, **28**, 475–488.

Penberthy, C.J. (1996). The use of SEM-based image analysis to investigate the extraction of platinum-group elements from the UG-2 Chromitite, Bushveld Complex. *In*: Niedbalska, A., Szymanski, A. and Wiewióra, A. (Eds.), *Proc. 5th Int. Congress Appl. Miner. Miners. Ind.*, Warsaw, 2–5 June 1996, 192–197.

Peyerl, W. (1982). The influence of Driekop Dunite Pipe on the platinum-group mineralogy of the UG-2 Chromitite in its vicinity. *Econ. Geol.*, **77**, 1432–1438.

Schiffries, C.M. and Rye, D.M. (1990). Stable isotopic systematics of the Bushveld Complex: II. Constraints on hydrothermal processes in layered intrusions. *Am. J. Sci.*, **290**, 209–245.

Schiffries, C.M. and Skinner, B.J. (1987). The Bushveld hydrothermal system: field and petrologic evidence. *Am. J. Sci.*, **287**, 566–595.

Shuttleworth, G. (1985a). Rustenburg's Pandora. *Finance Week*, 157–160.

Shuttleworth, G. (1985b). UG-2 reef comes of age. *Finance Week*, 741–742.

Shuttleworth, G. (1985c). Rustenburg to 'expand'. *Finance Week*, 652–654.

Van der Merwe, J.J., Vermaak, A.H., Slabbert, M.J., Mauve, A.C. and Mooney, D.J. (1998). An overview of the geology of the UG-2 Chromitite layer and its surrounding lithologies on Lonrho Platinum's lease area. *In*: *Abstr. 8th Int. Platinum Symp.*, June–July 1998, Rustenburg, S. Afr., Geol. Soc. S. Afr., S. Afr. Inst. Min. Metall., Symp. Ser. S18, 403–406.

Vaughan, D.J. and Craig, J.R. (1978). *Mineral Chemistry of Metal Sulphides*. Cambridge Univ. Press, Cambridge, England, 493 pp.

Vermaak, C.F. and Hendriks, L.P. (1976). A review of the mineralogy of the Merensky Reef, with specific reference to new data on the precious metal mineralogy. *Econ. Geol.*, 71, 1244–1269.

Verryn, S.M.C. and Merkle, R.K.W. (1994). Compositional variation of cooperite, braggite and vysotskite from the Bushveld Complex. *Mineral. Mag.*, **58**, 223–234.

Viljoen, M.J. and Hieber, R. (1986). The Rustenburg Section of Rustenburg Platinum Mines Limited, with reference to the Merensky Reef. *In*: Anhaeusser, C.R. and Maske, S. (Eds.), *Mineral Deposits of Southern Africa*. Geol. Soc. S. Afr., Johannesburg, S. Afr., **II**, 1107–1134.

Viljoen, M.J. and Scoon, R.N. (1985). The distribution and main geologic features of discordant bodies of iron-rich ultramafic pegmatite in the Bushveld Complex. *Econ. Geol.*, **80**, 1109–1128.

Viljoen, M.J., De Klerk, W.J., Coetzer, P.M., Hatch, N.P., Kinloch, E. and Peyerl, W. (1986a). The Union Section of Rustenburg Platinum Mines Limited with reference to the Merensky Reef. *In*: Anhaeusser, C.R. and Maske, S. (Eds.), *Mineral Deposits of Southern Africa*. Geol. Soc. S. Afr., Johannesburg, S. Afr., **II**, 1061–1090.

Viljoen, M.J., Theron, J., Underwood, B., Walters, B.M., Weaver, J. and Peyerl, W. (1986b). The Amandelbult Section of the Rustenberg Platinum Mines Limited, with reference to the Merensky Reef. *In*: Anhaeusser, C.R. and Maske, S. (Eds.), *Mineral Deposits of Southern Africa*. Geol. Soc. S. Afr., Johannesburg, S. Afr., **II**, 1041–1060.

Von Gruenewaldt, G. (1977). The mineral resources of the Bushveld Complex. *Miner. Sci. Eng.*, **9**, 83–95.

Von Gruenewaldt, G., Hatton, C.J., Merkle, R.K.W. and Gain, S.B. (1986). Platinum-group element–chromitite associations in the Bushveld Complex. *Econ. Geol.*, **81**, 1067–1079.

Von Gruenewaldt, G., Dicks, D., De Wet, J. and Horsch, H. (1990). PGE mineralization in the western sector of the eastern Bushveld Complex. *Miner. Petrol.*, **42**, 71–95.

Winkels-Herding, S., Merkle, R.K.W. and Von Gruenewaldt, G. (1991). Pegmatoidal pockets in the UG-2 Chromitite, western Bushveld Complex. *ICAM '91, Pap. Int. Congress Appl. Miner.*, Mineralog. Assoc. S. Afr., Pretoria, S. Afr., **2**, 1–14.

Editorial handling: R.G. Cawthorn.